Pseudo Optical PAM-*N* Signal Using Externally Modulated Lasers

Joon Young Huh, Joon Ki Lee, Sae-Kyoung Kang, and Jyung Chan Lee

We propose a pseudo optical *N*-level pulse-amplitude modulation (PO PAM-*N*) signal using a few externally-modulated lasers (EMLs) operating at different wavelengths, which is suitable for upgrading the transmission speed over an optical link of < 10 km single-mode fiber with low-cost components. To compare a PO PAM-*N* signal with that of a standard optical PAM-*N* signal, we perform experiments for evaluating the performance of a 51.56-Gb/s PO PAM-4 signal and standard 51.56-Gb/s optical PAM-4 signal. The receiver sensitivity (at BER = 10^{-5}) of the PO PAM-4 signal is 1.5 dB better than the receiver sensitivity of a standard optical PAM-4 signal. We also investigate the feasibility of PO PAM-*N* (*N* = 4, 8, and 16) signals operating at 103.12 Gb/s, considering relative intensity noise, timing jitter, extinction ratio (ER) of EMLs, and dispersion. From the results, a PO PAM-8 signal performs better than PO PAM-4 and PO PAM-16 signals at 103.12 Gb/s. Finally, we suggest a timing control method to suppress the effect of dispersion in a PO PAM-*N* signal. We show that the tolerance to dispersion of a 103.12-Gb/s PO PAM-8 signal can be improved to ±40 ps/nm by applying a proposed scheme.

Keywords: Pseudo optical PAM-*N*, Ethernet, modulation format, 100 GE, 400 GE.

Manuscript received June 23, 2014; revised Sept. 23, 2015; accepted Oct. 14, 2015.

This work was supported by the IT R&D program of MKE/KEIT (10041414, Terabit Optical-Circuit-Packet Converged Switching System Technology Development for Next-Generation Optical Transport Network).

Joon Young Huh (corresponding author, yurinara@etri.re.kr), Joon Ki Lee (juneki@etri.re.kr), Sae-Kyoung Kang (skkang35@etri.re.kr), and Jyung Chan Lee (jclee@etri.re.kr) are with the Communications Internet Research Laboratory, ETRI, Daejeon, Rep. of Korea.

I. Introduction

With the rapid proliferation of bandwidth-consuming applications such as cloud services, social networking, and smartphones, Internet traffic is growing explosively. To cope with this situation, there have been many efforts to increase the transmission capacity of a local-area network (LAN) for data center networks, financial networks, and Internet exchanges [1]–[4]. In developing a high-capacity transceiver module for short-range optical links not exceeding 10 km of single-mode fiber (SMF) such as LAN, the size and cost of the module are the most important factors to be considered, and are largely affected by the optical components used in the transceiver module. Thus, the number of optical channels should be minimized, and each channel should carry the highest possible transmission speed, while keeping the manufacturing and operating cost low. To satisfy this condition, many research groups have struggled to implement an *N*-level pulse-amplitude modulation (PAM-*N*) signal, because it can be easily generated with relatively low-cost components.

An optical PAM-*N* signal is typically generated by an electrical PAM-*N* signal [5]–[10]. An electrical PAM-*N* signal is synthesized by combining M (= $\log_2 N$) electrical non-return to zero (NRZ) signals using electrical amplifiers and combiners or an *M*-bit digital-to-analog converter (DAC). However, the quality of the combined signal is significantly degraded owing to the noise and linearity of the electrical components. Therefore, the feasibility of an optical PAM-*N* signal for a high speed such as beyond 100 Gb/s with commercial components has been difficult to show. Recently, there have been various efforts to generate a high-speed optical PAM-*N* signal of good quality [11]–[13].

In this paper, we propose a pseudo optical PAM-*N* signal (PO PAM-*N*) using M (= $\log_2 N$) externally-modulated lasers

http://dx.doi.org/10.4218/etrij.15.0114.0746

(EMLs) operating at different wavelengths. The signal is transmitted as a combination of NRZ signals with different wavelengths through the optical link. A photo detector (PD) receives all NRZ signals and generates an electrical PAM-N signal. We experimentally show that the quality of the PO PAM-N signal is better than in standard methods by comparing the performance of a standard 51.56-Gb/s optical PAM-4 signal and 51.56-Gb/s PO PAM-4 signal, since the PO PAM-4 signal does not require any linear electrical components.

To optimize a PO PAM-N signal (N = 4, 8, and 16) at 103.12 Gb/s, we have investigated the effects of the optical carrier frequency separation, the extinction ratio (ER) of the external modulators, the relative intensity noise (RIN), and the timing jitter among the EML characteristics through a VPI simulation. The representative transmission speed for future short-range optical links such as next-generation Ethernet is 103.12 Gb/s [2]. We assume that forward error correction (FEC) is implemented in a 103.12-Gb/s PO PAM-N signal. We have also investigated the effects of chromatic dispersion and frequency separation. To improve the tolerance to dispersion, we propose a timing control scheme. From these results, we examine the competitiveness of PO PAM-N signals with commercial components at 103.12 Gb/s.

II. Principle of Operation

Figure 1(a) shows a schematic of the proposed PO PAM-N signal with $N = 8$ using a few optical channels for short-range optical transmission. The ith (i = 1, 2, and 3) EML generates an optical NRZ signal of carrier frequency f_i. The three EMLs used in the generation of a PO PAM-8 signal have different frequencies, which are inside the bandwidth of the optical mux and demux shown in Fig. 1(b). The frequency separations should be larger than the bandwidth of the PD. The beating components fall outside of the bandwidth of the PD when the NRZ signals are detected, as shown in Fig. 1(c). Meanwhile, the optical NRZ signals are combined in a power ratio of 2^2:2:1 through appropriately adjusting signal power or the coupling ratio of the coupler. After the coupler, three NRZ signals pass through the transmission link, as shown in Fig. 1(d). After PD, the PO PAM-8 signal changes to a clean electrical PAM-8 signal, as shown in Fig. 1(e).

A PO PAM-N signal can be modelled through mathematical formulae. The optical field of the ith NRZ signal (i = 1, 2, … , M), with $M = \log_2 N$, used in this method is given by

$$\begin{aligned} E_1 &= A_1 \operatorname{Re}\{\exp[-i(2\pi f_1 t + \varphi_1)]\}, \\ E_2 &= A_2 \operatorname{Re}\{\exp[-i(2\pi f_2 t + \varphi_2)]\}, \\ &\vdots \\ E_M &= A_M \operatorname{Re}\{\exp[-i(2\pi f_M t + \varphi_M)]\}, \end{aligned} \tag{1}$$

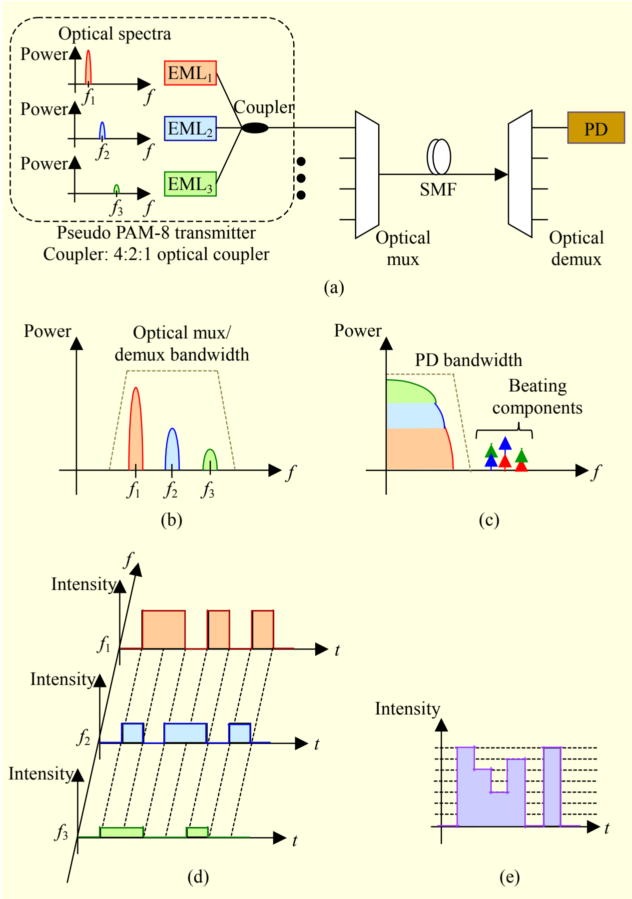

Fig. 1. Transmission of proposed PO PAM-8 signal: (a) schematic of transmission link using PO PAM-8 signal, (b) optical spectrum of PO PAM-8 signal before PD, (c) electrical spectrum of PO PAM-8 signal after PD, (d) PO PAM-8 signal in optical time domain after 4:2:1 optical coupler, and (e) PO PAM-8 signal in electrical time domain after PD.

where A_k, f_k, and ϕ_k (k = 1, 2, … , M), with $M = \log_2 N$, are the data information added to each EML, the optical carrier frequency, and the optical phase, respectively. Equation (2) below gives the electrical signal at the PD, after the optical fields are combined by the "$2^{(M-1)}$: ⋯ : 2 : 1" optical coupler.

$$P_{\text{rec}} = K\left|E_1 + \sqrt{2}E_2 + \cdots + \sqrt{2^{(M-1)}}E_M\right|^2, \tag{2}$$

where K is the responsivity of the PD. We obtain (3) through (1) and (2).

$$\begin{aligned} P_{\text{rec}} &= KA_1^2 + 2KA_2^2 + \cdots + 2^{M-1}KA_M^2 \\ &+ 2\sqrt{2}KA_1A_2\cos[2\pi(f_1 - f_2)t + \varphi_1 - \varphi_2] \\ &+ \cdots + \\ &2\sqrt{2^{(2M-3)}}KA_{M-1}A_M\cos[(f_{M-1} - f_M)t + \varphi_{M-1} - \varphi_M]. \end{aligned} \tag{3}$$

In (3), the sum from the first term to the Mth term is the desired

PO PAM-N signal. If the carrier frequency separations of the NRZ signals are set to be larger than the bandwidth of the PD, then the beating components are outside of the PD bandwidth and filtered out, as shown in Fig. 1(c), leaving a clean electrical PAM-N signal.

III. Experimental Results

To compare the performance of a PO PAM-N signal and standard optical PAM-N signal, we evaluate the performances of a 51.56-Gb/s PO PAM-4 signal and standard 51.56-Gb/s optical PAM-4 signal. Figure 2(a) shows the experimental setup to generate a standard 51.56-Gb/s optical PAM-4 signal. First, an electrical PAM-4 signal is generated using a 32 GBd 3-bit DAC and two 25.78-Gb/s NRZ signals (pattern length: $2^{11} – 1$). An optical PAM-4 signal is obtained from an electrical PAM-4 signal and an intensity Mach–Zehnder interferometric modulator. The bandwidth and extinction ration of the intensity modulator is 22 GHz and 13 dB, respectively. The optical signal is sent to a PD, and then sampled through a digital sampling oscilloscope (DSO) at 50 GS/s. The electrical bandwidth is limited to 18 GHz by the DSO. The sampled data are processed offline for the bit-error rate (BER) estimation using direct error counting. Figure 2(b) shows the experimental setup for the generation of a 51.56-Gb/s PO PAM-4 signal. Two lasers are modulated with 25.78-Gb/s NRZ signals (pattern length of $2^{11} – 1$). We utilize two commercial EMLs, the EO bandwidths of which are 18 GHz. The wavelengths of the lasers are 1,304.5 nm and 1,309 nm. We combine the modulated signals using a 67%/33% coupler for the PO PAM-4 signal. The BERs of the signal are measured with and without 10 km SMF through off-line processing. Figure 2(c) shows the measured BER curves of the standard optical PAM-4 signal and the PO PAM-4 signal. The receiver sensitivity (for a BER of 10^{-5}) of the PO PAM-4 signal is better by about 1.5 dB than the standard optical PAM-4 signal because the linear electrical components are not used in the PO PAM-4. The improvement can be increased with an operating signal speed such as 103.12 Gb/s. The insets in Fig. 2(c) show the eye diagrams of a standard optical PAM-4 signal and PO PAM-4 signal. The PO PAM-4 signal has a cleaner eye compared to the standard signal. We also archived the BER of the PO PAM-4 signal after 10 km SMF without less power penalty compared to a back-to-back operation through a timing controlling method. This is explained in detail in Section VI.

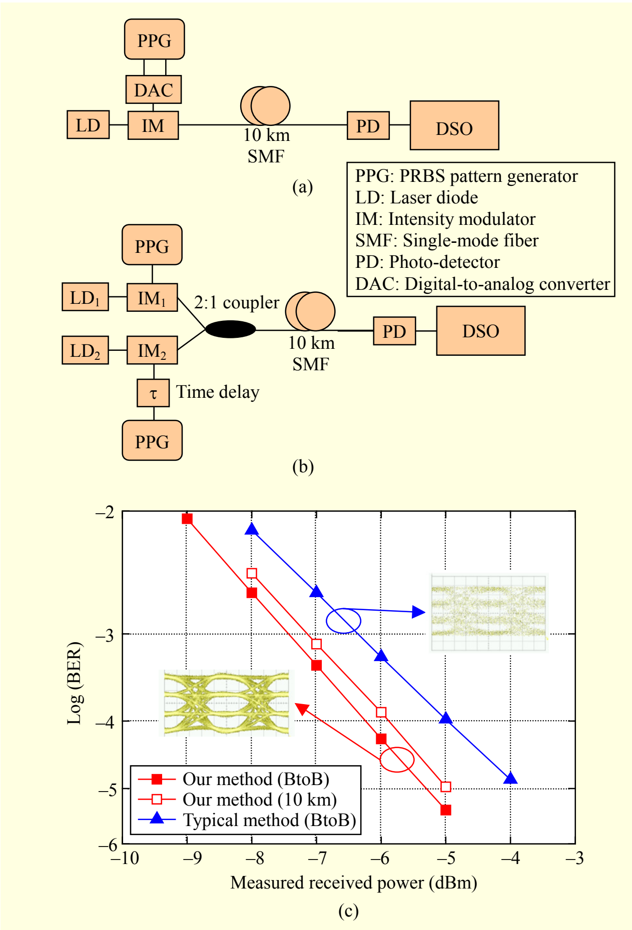

Fig. 2. (a) Experimental setup of standard 51.56-Gb/s optical PAM-4 signal, (b) experimental setup of 51.56-Gb/s PO PAM-4 signal, and (c) measured BER curves of standard optical PAM-4 signal and PO PAM-4 signal at 51.56 Gb/s.

IV. Simulation Setup

To compare the performance of various PO PAM-N signals, we have performed a simulation through a software of VPIsystems for 103.12-Gb/s PO PAM-N signals (N = 4, 8, and 16) using the setup shown in Fig. 3. For the generation of the PO PAM-N signals (N = 4, 8, and 16), we use two, three, and four EMLs, respectively, and modulate the EMLs with a 51.56-Gb/s NRZ, 34.37-Gb/s NRZ, and 25.78-Gb/s NRZ (pattern length of $2^{11} − 1$), respectively. In Fig. 3, the wavelength of EML_1 is 1,310 nm, and the frequency separations of the neighboring EMLs are 100 GHz. We combined the modulated signals using a 2:1, 4:2:1, and 8:4:2:1 coupler for the PO PAM-N signals (N = 4, 8, and 16), respectively. After the transmission of the PO PAM-N signals, an error detector measures the BER, where the thermal noise and shot noise are taken into account deterministically [10].

We analyze how the EML characteristics affect the performance of the PO PAM-N signal generation. We set the ER, RIN, timing jitter, frequency separation of the EMLs, the thermal noise of the PD, and the input referred noise of the trans-impedance amplifier (TIA) to be 13 dB [14], –150 dB/Hz

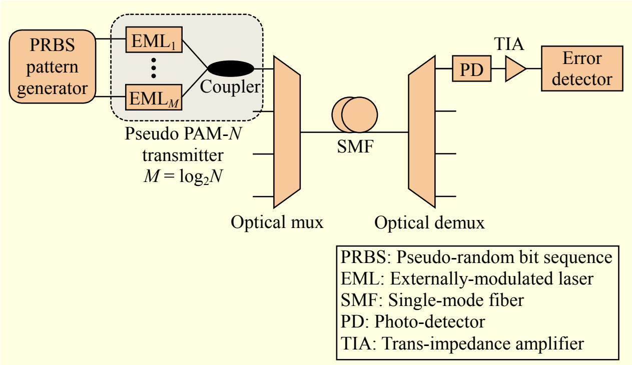

Fig. 3. Simulation setup of PO PAM-N ($N = 4$, 8, and 16) signals.

[15], 1.5 ps [16], 100 GHz, 25 pA/(Hz)$^{1/2}$ [16], and 2 μA(rms) [16], respectively. The receiver sensitivity is measured when the BER is 10^{-5} because of the FEC [10].

First, we simulate the effects of the EML, PD, and TIA bandwidths for the PO PAM-N signals ($N = 4$, 8, and 16) at 103.12 Gb/s. From the results, we obtain the optimum bandwidth of the components for the PO PAM-N signals. Additional simulations are performed while setting the optimum bandwidths. To analyze the effect of the ERs of the EMLs, we simulate the receiver sensitivity of the PO PAM-N signals ($N = 4$, 8, and 16), while changing the ERs and fixing the other parameters. We also investigated the effects of the RIN, timing jitter, and frequency separation of the EMLs in the same way. The simulation results of the PO PAM-N ($N = 4$, 8, and 16) signals at 103.12 Gb/s are compared to those of a 25.78-Gb/s NRZ signal, which is widely used for short-range optical transmission links such as Ethernet-based LAN [1]–[4].

V. Optimization of PO PAM-N Signal

We first investigate the effect of the receiver and transmitter bandwidth on the PO PAM-N ($N = 4$, 8, and 16) signals, whose symbol rates are 51.56 Gsymbol/s, 34.37 Gsymbol/s, and 25.78 Gsymbol/s, respectively. The receiver bandwidth is defined as the combination of TIA and PD bandwidths. The transmitter bandwidth is the bandwidth of the EML. For the investigation, we use a receiver bandwidth ratio (RBR) and transmitter bandwidth ratio (TBR) to remove the effect of the symbol rate. The RBR and TBR are defined as the ratio of the receiver bandwidth to the symbol rate, and the ratio of the transmitter bandwidth to the symbol rate, respectively.

Figure 4 shows the receiver sensitivities (for a BER of 10^{-5}) as a function of RBR, for different values of TBR. It is observed that the minimum receiver sensitivities are decreased with the TBRs. We set the optimum points to be within 0.5 dB of the minimum receiver sensitivities. For the 25.78-Gb/s NRZ and 103.12-Gb/s PO PAM-N signals ($N = 4$, 8, and 16), the optimum TBRs and RBRs are (0.8, 0.75), (1.0, 0.9), (1.1, 1.05), and (1.2, 1.2), respectively. The eye diagrams shown in the insets of Fig. 4 are electrically measured at optimum points of the PO PAM-N signals. In Fig. 4, the optimum RBR and TBR of the PO PAM-N signals are larger than in the NRZ signal. This is because the number of transient paths (for example, the paths from 0-level to 1-level, from 0-level to 2-level, ··· , and from (N – 2)-level to (N – 1)-level) is significantly increased with the N in the PO PAM-N signals. The high-frequency components are increased with increasing N.

In additional simulations, we use the optimum transmitter and receiver bandwidths obtained above. The optimum RBRs and TBRs are not affected much by the EML characteristics, such as the ER, RIN, and timing jitter, because the characteristics of the parameters are almost independent of the signal bandwidth.

The frequency separations between the EMLs are very important factors in PO PAM-N signals, because it affects how much the PD can eliminate the beating components, as shown in Fig. 1(c). Figure 5(a) shows the power penalties of the PO PAM-N ($N = 4$, 8 and, 16) signals, while changing the frequency separations between neighboring EMLs. The power penalties are measured compared to the receiver sensitivities (for BERs of 10^{-5}) at a 400 GHz frequency separation in the PO PAM-N signals. When the frequency separations are below 100 GHz, we found that large power penalties occurred. This is because the beating component passes through the receiver. However, when it is larger than 100 GHz, there is a negligible power penalty. In addition, the frequency of each EML can be easily manipulated with the temperature control [17].

We also investigate the effect of the EMLs' ERs. Figure 5(b) shows the receiver sensitivities of the 25.78-Gb/s NRZ signal and 103.12-Gb/s PO PAM-N ($N = 4$, 8, and 16) signals when the BERs are 10^{-5}, while changing the ERs of the EMLs in the generation of the PO PAM-N signals. From the results, it is possible to generate 103.12-Gb/s PO PAM-N ($N = 4$, 8, and 16) signals within respectively 8.1 dB, 10.4 dB, and 14.3 dB penalties compared to the 25.78-Gb/s NRZ signal when the ERs of the EMLs are 13 dB (to suppress the ER effect). The main reason for the power penalties is that the signal-to-noise ratio (SNR) between the (N – 1)-level and (N – 2)-level of a PO PAM-N signal is significantly decreased with N. Thus, the SNR degradation is more dominant than the effect of the increase in the symbol rate. From the results, we found that the receiver sensitivities of the PO PAM-4 signal and the PO PAM-8 signal at 103.12 Gb/s are obtained at below –6 dBm when the ERs are 13 dB, and it is difficult to obtain a high quality PO PAM-16 signal.

In a PO PAM-N signal, the RINs of the EMLs is a critical parameter for the signal quality, because RIN directly affects

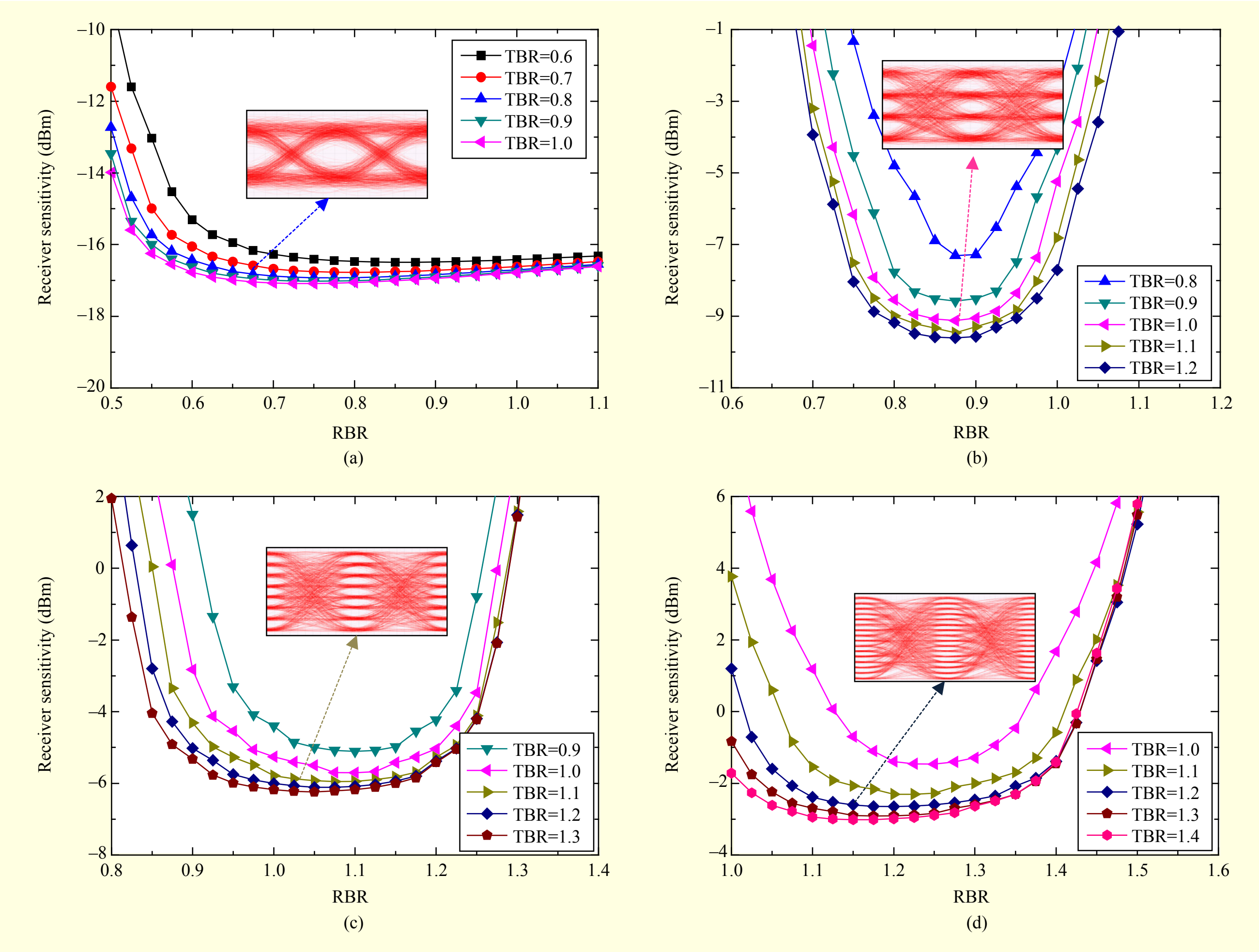

Fig. 4. Effect of RBRs and TBRs for (a) 25.78-Gb/s NRZ signal, (b) 103.12-Gb/s PO PAM-4 signal, (c) 103.12-Gb/s PO PAM-8 signal, and (d) 103.12-Gb/s PO PAM-16 signal.

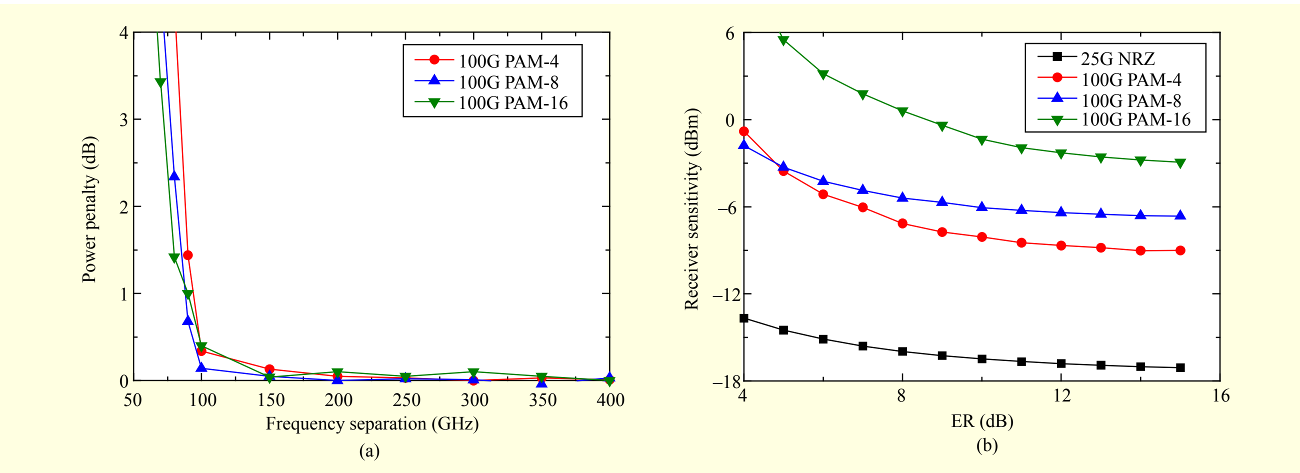

Fig. 5. Effects of EML characteristics on qualities of PO PAM-N signals (N = 4, 8, and 16): (a) effect of frequency separations between EMLs and (b) effect of ER of EMLs.

SNR. For the investigation, we simulated the power penalties of a 25.78-Gb/s NRZ signal and 103.12-Gb/s PO PAM-N (N = 4, 8, and 16) signals, while changing the RINs of the EMLs. The power penalties are measured compared to the receiver

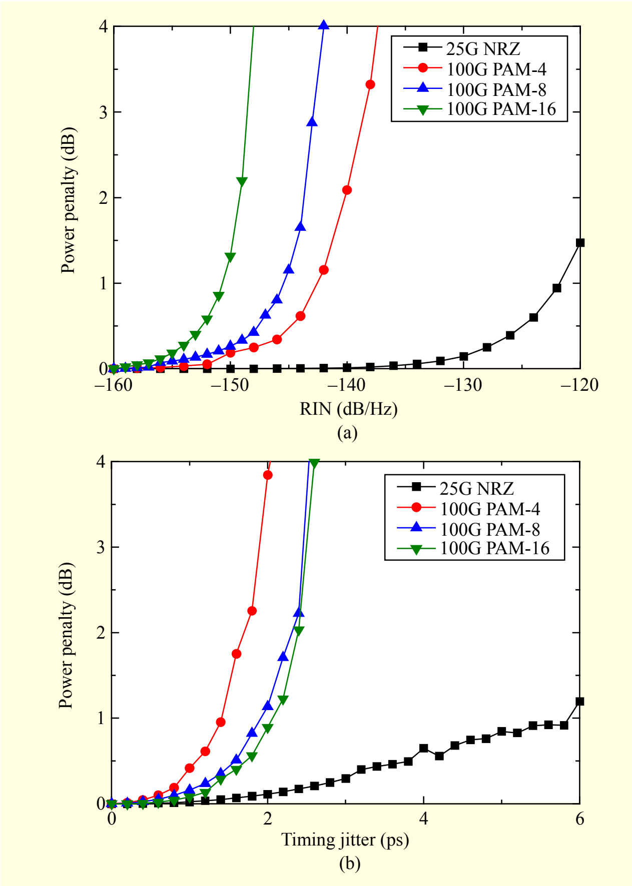

Fig. 6. Effects of EML characteristics on qualities of PO PAM-N signals: effect of (a) RINs and (b) timing jitter of EMLs.

sensitivities (for BERs of 10^{-5}), when the RINs of the EMLs are –160 dB/Hz in PO PAM-N signals.

Figure 6(a) shows that the effects of the RIN are increased with N. The PO PAM-16 signal is significantly affected by the RIN compared to the NRZ signal, although they had the same symbol rate. This is because the high RIN degraded the SNR of the eye opening between the (N – 1)-level and (N – 2)-level in the PO PAM-N signals. The small eye opening caused by the increment of N aggravated the effect of RIN. The RIN limitation points within a 0.5 dB penalty of the 25.78-Gb/s NRZ signal and 103.12-Gb/s PO PAM-N (N = 4, 8, and 16) signals are –124 dB/Hz, –142 dB/Hz, –147 dB/Hz, and –151 dB/Hz, respectively. Therefore, the PO PAM-4 and PO PAM-8 signals at 103.12 Gb/s have an acceptable power penalty because the RIN of the commercial laser diode is approximately –150 dB/Hz [11].

The timing jitter of the EMLs is also an important parameter for the quality of a PO PAM-N signal because the width of the transient region increases with the timing jitter and the effective SNR decreases accordingly. The power penalties of the PO PAM-N signals as a function of the timing jitter are shown in Fig. 6(b). The power penalties are referred to the receiver sensitivities for BERs of 10^{-5} when the timing jitters of the EMLs are 0 ps in the PO PAM-N signals. The timing jitter for a 0.5 dB penalty of the NRZ signal and PO PAM-N (N = 4, 8, and 16) signals are 4 ps, 1.1 ps, 1.6 ps, and 1.8 ps, respectively. We found that the PO PAM-4 signal had the lowest tolerance in terms of the timing jitter because the PO PAM-4 signal had a smaller transient path region owing to the high speed of the signal's symbol rate (approx. 51.56 Gsymbol/s) — higher than the other PO PAM-N signals. However, the tolerance of the PO PAM-16 signal is smaller than that of the NRZ signal, although they had the same symbol rate. This is because the effective transient region is also affected by the number of transient paths of the PO PAM-N signal. From the results, we found that the PO PAM-N signals except the PO PAM-4 signal at 103.12 Gb/s satisfied the timing jitter condition of >1.5 ps [13].

From the simulation results for ERs and RINs, we note that both the PO PAM-4 signal and the PO PAM-8 signal at 103.12 Gb/s can be implemented using commercial components. However, if we include the effect of the timing jitter, only the PO PAM-8 signal at 103.12 Gb/s satisfies the requirements for a short-range optical transmission, such as Ethernet.

VI. Limitation of Chromatic Dispersion

The quality of the PO PAM-N signal is affected by chromatic dispersion because the EMLs in the signal generation have different wavelengths. Figure 7(a) shows a schematic of the SMF-based transmission link using a PO PAM-4 signal. Figure 7(b) shows a PO PAM-4 signal using two EMLs operating at different wavelengths before transmission (at point 1). After transmission (at point 2), the NRZ signals from the two EMLs have a time difference (Δτ) caused by the chromatic dispersion of the optical link, as shown in Fig. 7(c). As a result, the electrical PAM-4 signal after PD (at point 3) is broken owing to the time delay between the signals of the EMLs, as shown in Fig. 7(d). To address this problem, we propose the application of a timing control at the EMLs. The time delay (Δτ) between the EML signals can be easily precalculated by considering the link length, frequency separation, and chromatic dispersion of the transmission link. Thus, if the time delay (Δτ) is applied to the EMLs with opposite sign, as in Fig. 7(e), then the effect of the chromatic dispersion and frequency difference after transmission (at point 2) is removed effectively, as shown in Fig. 7(f). As a result, a *clean* electrical PAM-4 signal is obtained after the PD (at point 3), such as in Fig. 7(g). This method can be easily applied using the electrical timing control of the EMLs because the timing control is already implemented through common transceiver modules

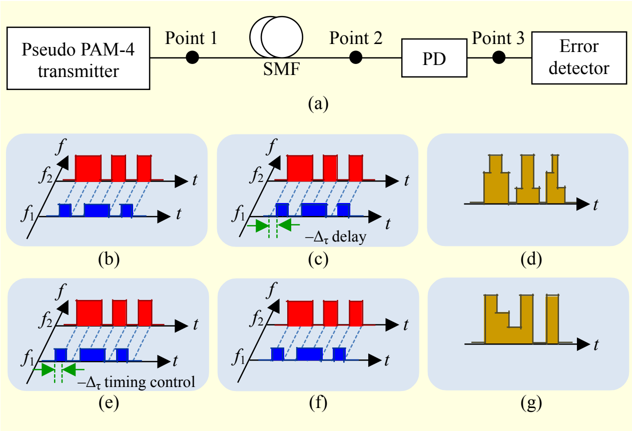

Fig. 7. Timing control method to compensate for chromatic dispersion for PO PAM-4 signal: (a) schematic of optical transmission link using PO PAM-4 signal, (b) PO PAM-4 signal at point 1 without timing control scheme, (c) PO PAM-4 signal at point 2 without timing control scheme, (d) PO PAM-4 signal at point 3 without timing control scheme, (e) PO PAM-4 signal at point 1 with timing control scheme, (f) PO PAM-4 signal at point 2 with timing control scheme, and (g) PO PAM-4 signal at point 3 with timing control scheme.

such as a 100 GE CFP transceiver [14].

To verify this method, we investigated the effect of the chromatic dispersion and frequency separation with and without a timing control method. First, we simulated the power penalties of the PO PAM-8 signal at 103.12 Gb/s, while changing the chromatic dispersion of the transmission link when the frequency separations of neighboring EMLs are 100 GHz. The power penalties are measured and compared to the receiver sensitivities of the PO PAM-8 signal (for BERs of 10^{-5}), when the chromatic dispersion is 0 ps/nm in the optical link. In Fig. 8(a), the tolerance to dispersion (within a 1 dB power penalty) without a timing control is only ±8 ps/nm. However, the effect of the chromatic dispersion and frequency separation in the PO PAM-8 signal could be removed by the timing control between EMLs, as shown in Figs. 7(f) and 7(g). As a result, the tolerance to dispersion of the PO PAM-8 signal is improved to ±40 ps/nm. We also performed simulations for a 103.12-Gb/s PO PAM-8 signal with the timing control scheme when the frequency separations are 200 GHz and 400 GHz. As a result, the tolerance to dispersion for each frequency separation is also improved in the same way, as shown in Fig. 8(a). That is, it is possible to apply the timing control scheme regardless of the frequency separation.

The chromatic dispersion also affects the PO PAM-N signal individually. Thus, we investigated the effect of chromatic dispersion on the PO PAM-N signal with a timing control. Figure 8(b) shows the power penalties of the 25.78-Gb/s NRZ signal and the PO PAM-N signals (N = 4, 8, and 16) at

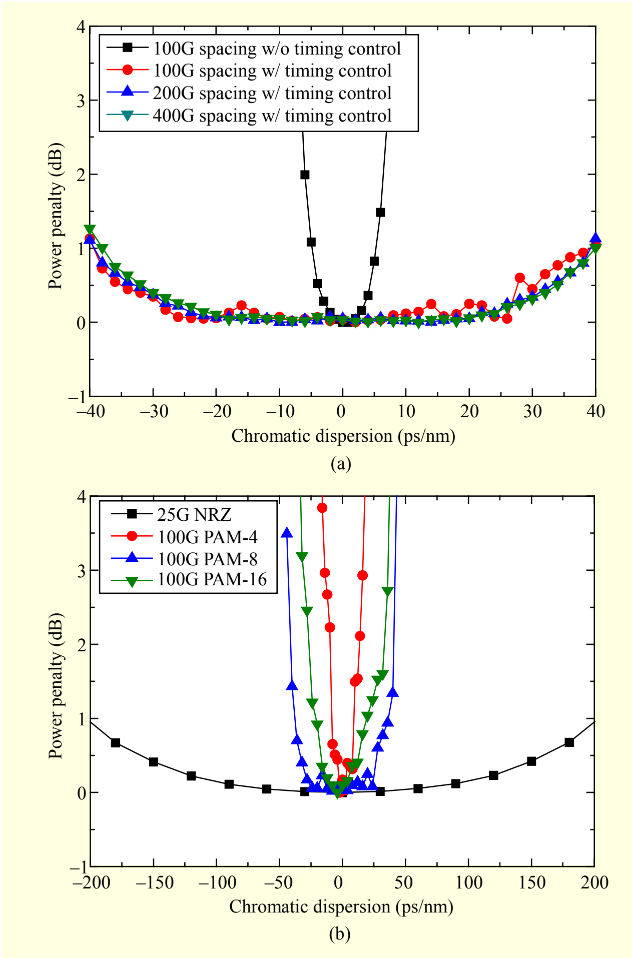

Fig. 8. (a) Comparison of chromatic tolerance to dispersion of 103.12-Gb/s PO PAM-8 signal w/ and w/o timing control scheme and (b) effect of chromatic dispersion on PO PAM-N signals (N = 4, 8, and 16) w/ timing control scheme.

103.12 Gb/s with the timing control when the frequency separation is set to 100 GHz. The power penalties are measured in comparison to the receiver sensitivities of the signals (for BERs of 10^{-5}), when the chromatic dispersion is 0 ps/nm in the optical link. In Fig. 8(b), the tolerances to dispersion (within 1 dB power penalty) are ±220 ps/nm, ±9 ps/nm, ±40 ps/nm, and ±28 ps/nm for the NRZ signal and the PO PAM-N (N = 4, 8, and 16) signals, respectively. The symbol rate of the PO PAM-N signal, which is directly related to the bit period of the signal, is a very dominant factor for the tolerance to dispersion. Thus, the 103.12-Gb/s PO PAM-4 signal had very low tolerance to dispersion of ±9 ps/nm, since it had the largest symbol rate among the 103.12-Gb/s PO PAM-N (N = 4, 8, and 16) signals. However, the PO PAM-16 signal had a much lower tolerance to dispersion than the NRZ signal, although they had the same symbol rates. This is because the PO PAM-16 signal had a wider effective bandwidth than the NRZ signal owing to the many transition paths of the PO PAM-16 signal. As a result, we found that only the 103.12-Gb/s PO PAM-8 signal had a sufficient tolerance to dispersion (at ±40 ps/nm) for short-range optical links.

VII. Conclusion

We proposed and theoretically investigated a PO PAM-N signal using M (= $\log_2 N$) EMLs operating at different wavelengths. The PO PAM-N signal was received as a PO PAM-N signal after the PD without the need to electrically combine NRZ signals. Therefore, it is possible to realize a *clean* PO PAM-N signal at high speed (over 100 Gb/s) because, contrary to a standard optical PAM-N signal, the realized signal is only slightly affected by the electrical noise and linearity of the components. To verify the potential of the proposed method, we experimentally showed that the receiver sensitivity (for BER of 10^{-5}) of a 51.56-Gb/s PO PAM-4 signal was 1.5 dB better than the receiver sensitivity of a standard optical PAM-4 signal.

To verify the feasibility of the PO PAM-N signals operating at 103.12 Gb/s, we also investigated the optimum transmitter bandwidth, the optimum receiver bandwidth, the RIN limitation, the timing jitter limitation, and the tolerance to dispersion. In the case of a 103.12-Gb/s PO PAM-8 signal, the optimum ratios of the transmitter and receiver bandwidth to the symbol rate are 1.1 and 1.05, respectively. The RIN for a 0.5 dB penalty is –147 dB/Hz, and the timing jitter for a 0.5 dB penalty is 1.6 ps. Therefore, we have shown that the PO PAM-8 signal at 103.12 Gb/s can be easily implemented through commercial components. In addition, the proposed timing control method improves the tolerance to dispersion of a 103.12-Gb/s PO PAM-8 signal from ±8 ps/nm to ±40 ps/nm. This suggests that the PO PAM-4 signal, with appropriately manipulating the wavelength of lasers, is a possible solution for a 400-Gb/s short-range optical link not exceeding approximately 10 km SMF.

References

[1] IEEE STANDARDS ASSOCIATION, *IEEE P802.3bm 40 Gb/s and 100 Gb/s Fiber Opt. Task Force*. Accessed Oct. 21, 2015. http://www.ieee802.org/3/bm/public/index.html

[2] IEEE STANDARDS ASSOCIATION, *IEEE P802.3bs 400 Gb/s Ethernet Task Force*. Accessed Oct. 21, 2015. http://www.ieee802.org/3/bs/public/index.html

[3] S.-K. Kang et al., "A Cost-Effective 40 Gb/s ROSA Module Employing Compact TO-CAN Package," *ETRI J.*, vol. 35, no. 1, Feb. 2013, pp. 1–6.

[4] P.J. Winzer, "Beyond 100G Ethernet," *IEEE Commun. Mag.*, vol. 48, no. 7, July 2010, pp. 26–30.

[5] J.L. Wei et al., "Comparison of 100 Gb/S Ethernet Links Using PAM-8, Multipulse, and Hybrid CAP-16/QAM-16 Modulation Schemes," *European Conf. Exhibition Opt. Commun.*, London, UK, Sept. 22–26, 2013, pp. 1–3.

[6] K. Szczerba et al., "Intersymbol Interference Penalties for OOK and 4-PAM in Short-Range Optical Communications," *Opt. Fiber Commun. National Fiber Opt. Eng. Conf.*, Anaheim, CA, USA, Mar. 17–21, 2013, pp. 1–3.

[7] M.N. Sakib and O. Liboiron-Ladouceur, "A Study of Error Correction Codes for PAM Signals in Data Center Applications," *Photon. Technol. Lett.*, vol. 25, no. 23, Dec. 2013, pp. 2274–2277.

[8] A. Dochhan, M.O. Al-Dwairi, and W. Rosenkranz, "Optimization of Cost Efficient Multilevel-ASK Modulation Formats under the Constraint of Chromatic Dispersion," in *Proc. Opt. Fiber Commun. National Fiber Opt. Eng. Conf.*, San Diego, CA, USA, Mar. 21–25, 2010, p. OMJ7.

[9] F. Karinou et al., "IM/DD vs. 4-PAM Using a 1,550 nm VCSEL over Short-Range SMF/MMF Links for Optical Interconnects," in *Proc. Opt. Fiber Commun. National Fiber Opt. Eng. Conf.*, San Diego, CA, USA, Mar. 17–21, 2013, p. OW4A.2.

[10] G. Nicholl and C. Fludger, "Update on Technical Feasibility for PAM Modulation," *IEEE 802.3 NG 100 GE PMD Study Group*, Mar. 2012.

[11] M. Poulin et al., "107 Gb/s PAM-4 Transmission over 10 km Using a SiP Series Push-Pull Modulator at 1,310 nm," *European Conf. Opt. Commun., Exhibition*, Cannes, France, Sept. 21–25, 2014, pp. 1–3.

[12] M. Chagnon et al., "Experimental Study of 112 Gb/s Short Reach Transmission Employing PAM Formats and Sip Intensity Modulator at 1.3 µm," *Opt. Exp.*, vol. 22, no. 17, Aug. 2014, pp. 21018–21036.

[13] M.I. Hayee et al., "Doubling of Bandwidth Utilization Using Two Orthogonal Polarizations and Power Unbalancing in a Polarization-Division-Multiplexing Scheme," *Photon. Technol. Lett.*, vol. 13, no. 8, Aug. 2001, pp. 881–883.

[14] C. Sun et al., "Fabrication and Packaging of 40-Gb/s AlGaInAs Multiple-Quantum-Well Electro-absorption Modulated Lasers Based on Identical Epitaxial Layer Scheme," *J. Lightw. Technol.* vol. 26, no. 11, June 2008, pp. 1464–1471.

[15] Sumitomo Electronics, "Optical Transmission Components," 2012. Accessed Dec. 1, 2014. http://www.sedi.co.jp/products/optical_devices/index.html?version=en

[16] A. Ghiasi and B. Welch, "Investigation of 100 GbE Based on PAM-4 and PAM-8," *IEEE 802.3bm 40 Gb/s & 100 Gb/s Fiber Opt. Task Force*, Sept. 2012.

[17] Sumitomo Electronics, "100 Gb/s CFP Optical Transceiver Module SCF1001/1001L4 Series," 2013. Accessed Dec. 1, 2014. http://www.sedi.co.jp/ pdf/TMD14-039_SCF1001_1011L4.pdf

Joon Young Huh received his BS, MS, and PhD degrees in electrical engineering from the Korea Advanced Institute of Science and Technology, Daejeon, Rep. of Korea, in 2002, 2004, and 2010, respectively. In 2010, he joined ETRI. He is currently working on optical nonlinearity, advanced modulation formats, and next-generation Ethernet transceivers.

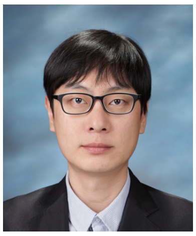

Joon Ki Lee received his BS degree in material engineering from Sungkyunkwan University, Suwon, Rep. of Korea, in 1995 and his MS degree in communication engineering from the Gwangju Institute of Science and Technology, Gwangju, Rep. of Korea, in 1997. He joined ETRI in 2001 and has worked on high-speed Ethernet transceivers and optical devices. He is the director of the optical transmission research section in ETRI.

Sae-Kyoung Kang received his PhD degree in electrical engineering from the Korea Advanced Institute of Science and Technology, Daejeon, Rep. of Korea, in 2006. In 2006, he joined ETRI, where he is currently working on high-speed Ethernet transceivers, optoelectronic packaging, and silicon photonic devices.

Jyung Chan Lee received his MS degree in electronics engineering from Hanyang University, Seoul, Rep. of Korea, in 1999. From February 1997 to February 1999, he was a student research associate at the Korea Institute of Science and Technology, where he worked on high-speed very short pulse generation from fiber ring lasers and erbium-doped fiber amplifiers. From March 1999 to May 2015, he worked at ETRI. As a researcher and director, at ETRI, he has participated in several research framework projects on photonic technologies and optical transceivers to communication systems and networks. Since June 2015, he has been acting as senior vice president and CTO at Optella Inc., an ETRI spin-off company, and has been manufacturing optical engines capable of 100 Gb/s and 400 Gb/s optical interconnectivity. His current research interests include high-speed arrayed optical engines applicable to optical transceivers and consumer devices; electronic equalization; CMOS photonics; and OTDR.

http://dx.doi.org/10.4218/etrij.15.0114.0746